Nanofibrous carbon (multi-wall carbon nanotubes): synthesis and electrochemical studies by using field-effect transistor setup

Ildar A. Mustafin [a] [iD], Arslan F. Akhmetov [a] [iD], Renat B. Salikhov [b] [iD], Ilnur A. Mullagaliev [b] [iD], Timur R. Salikhov [b] [iD], Rail N. Galiakhmetov [c], Olga V. Shabunina [d], Dmitry S. Kopchuk [de] * [iD], Igor S. Kovalev [d] [iD], Akhat G. Mustafin [c]

a: Department of Oil and Gas Technology, Ufa State Petroleum Technological University, Ufa 450062, Russia

b: Department of Infocommunication Technologies and Nanoelectronics, Ufa University of Science and Technology, Ufa 450076, Russia

c: Department of Physical Chemistry and Chemical Ecology, Ufa University of Science and Technology, Ufa 450076, Russia

d: Ural Federal University, Ekaterinburg 620002, Russia

e: I. Ya. Postovsky Institute of Organic Synthesis, Ural Branch of the RAS, Ekaterinburg 620009, Russia

* Corresponding author: d.s.kopchuk@urfu.ru

This paper belongs to a Regular Issue.

Abstract

Synthesis of nanofibrous carbon (multi-wall carbon nanotubes, MWCNTs) by means of *n*-hexane pyrolysis is reported. The structure of the obtained MWCNTs was studied using scanning electron microscopy, and the diameters of 20–85 nm and lengths of 500–600 nm for these nanotubes were observed. By using the above mentioned MWCNTs field-effect transistors were fabricated on ITO glass substrates with a gate dielectric made of 390 nm thick Al_2O_3 foil and the drain-source contacts made of 300 nm thick aluminum foil. The Nano-C film 200 nm thick was deposited by thermal evaporation in vacuum. The properties of the obtained field-effect transistors were studied. The current-voltage characteristics of the OFET show an increase in currents with a positive voltage on the gate, which corresponds to the electron conductivity of the transport channel. The dependences are nonlinear, and there are no saturation regions in the output characteristics. The Raman spectra indicate the presence of nickel and show characteristic peaks for C=C and CH bonds.

Key findings

● An effective method for the preparation of nanofibrous carbon (multi-wall carbon nanotubes, MWCNTs) is reported; the structure of the obtained MWCNTs was confirmed by means of physical methods.

● According to the SEM data, the diameter of the nanotubes is 20–85 nm and the length is 500–600 nm.

● By using the obtained MWCNTs, the samples of field-effect transistors were created, and charge carrier mobility as high as 0.008 cm² V⁻¹ s⁻¹ was observed.

1. Introduction

In recent decades, there has been a dramatic increase in the number of scientific works on the development of synthesis methods for the preparation of carbon materials (CMs) and studies of their properties. This is mainly due to the creation of various porous materials formed by mixed (transition) forms of carbon. These substances are of practical importance as adsorbents, catalysts, catalyst carriers, electrode components, paints, etc. [1]. Also, carbon materials, in particular carbon fibers (CFs), can replace traditional materials (for example, metals) in the form of composites [2]. Currently, new approaches are being developed to analyze the chemical state and reactivity of the carbon surface [3, 4]. In
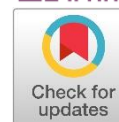
[5–10], various industrial fibrous carbons were sorted, and their morphological, physical and structural properties were carefully characterized.

Synthesis of CMs is a rather complex technological process, which involves using special equipment, high temperatures and expensive catalysts. In most cases, low molecular weight hydrocarbons are used as starting materials. And their pyrolysis at temperatures of 750–1200 °C at an atmospheric pressure produces molecular hydrogen and pyrolysis coke [11] according to the equation below:

$$2C_nH_m \rightarrow mH_2 + 2nC \qquad (1)$$
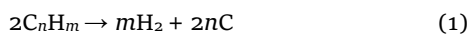
In the presence of catalysts [12–19] the same transformation takes place at much lower temperatures (500–800 °C). In addition, depending on the nature of the catalyst, nanofibrous carbon (NFC)/carbon nanotubes (CNTs) are formed during the reaction.

In this process, the catalysts consist of small-sized particles of transition metals, such as nickel, iron, cobalt *etc.*, which are formed *in situ* from the corresponding inorganic salts under the magnetron, electrobeam and cathode evaporation, chemical deposition from solutions or by chemical reduction of the corresponding metal salts. The studies of the mechanism of nanotube formation, as well as reaction conditions affecting the structure of materials were reported in several articles [20–23]. Obviously, to make the process of nanotube formation efficient and inexpensive, low-cost catalysts need to be used. It has been established that the temperatures of the process may vary significantly depending on the nature/composition of the catalyst. Some typical examples are presented below (Table 1).

It should be noted that the catalyst preparation procedure is quite complex. In this regard, the purpose of this work is to develop an effective method for producing carbon materials by using nickel (II) organic salts and to study the properties of the obtained materials. To accomplish this goal, instead of a pre-prepared nickel catalyst, we use a precursor of such catalyst, namely, readily accessible and cheap nickel 2-ethylhexanoate (2-EGN), which decomposes in a hydrocarbon media upon heating to form nanosized nickel particles [32]. These *in situ* formed nickel nanoparticles effectively catalyzed the formation of carbon nanotubes and allowed the reaction to be carried out at $T = 500$ °C. It worth to mention that the affordable method for obtaining 2-EGN was developed by us previously [33].

Table 1 Most common catalysts and process temperatures for the nanotube formation.

Raw materials	Conditions	Ref.	Raw materials	Conditions	Ref.
15% Fe/SiO$_2$	800 °C	[24]	40% Ni/SiO$_2$	500 °C	[28]
75% Co/Al$_2$O$_3$	500 °C	[25]	5% Ni/Al$_2$O$_3$	500 °C	[29]
62% Fe+8% Co/Al$_2$O$_3$	625 °C	[26]	75% Ni-15% Cu/Al$_2$O$_3$	675 °C	[30]
90% Ni/SiO$_2$	600 °C	[27]	37% Pd/Ni	725 °C	[31]

2. Experimental part

Elemental analysis was performed on a Sundy SDCHN636 CHN analyzer (China). SEM energy-dispersive X-ray spectra were collected using a TESCAN MIRA Scanning Electron Microscope (Chech Republic) with an energy dispersive microanalysis system AZteclive Lite Xplore 30 installed. The thickness of the layers in the field effect transistor was determined with a scanning probe microscope Nanoeducator II. Raman spectra were obtained using a M532/785 Raman microscope at 300 K (532 nm). The composition of the exhaust gases and unreacted carbon material (hexane part) was analyzed using a hardware-software complex "Chromatek Crystal 500" (JSC SKB Chromatek, Russia) and a gas chromatography-mass spectrometer Shimadzu GCMS-QP2020 (Japan). For the fabrication of electrodes a thermal vacuum deposition approach was used with an universal vacuum post UVP-250. The current-voltage characteristics of the obtained transistors were measured on a test stand consisting of a DC power supply HY3005D-2 and a DMM4020 multimeter as an ammeter. For the fabrication of films from solutions a CM-6M centrifuge was used.

2.1. Laboratory method for obtaining carbon materials (MWCNTs)

Experiments on obtaining MWCNs were carried out on a laboratory setup presented below (Figures 1 and S1 (enlarged)). The laboratory setup is made of heat-resistant glass P-15 «Pyrex». The process was carried out at a temperature of 500 °C; the feed rate of raw material, such as a reagent grade hexane (supplier JSC «EKOS» (Russia)), during the entire process was 50 mL/h. And 40% solution of 2-EGN in hexane obtained as described in literature [33] was used as a catalyst precursor. The catalyst for the process was prepared *in situ* in the amount equal to the 0.1 g of Ni.

In a typical procedure the catalyst precursor in a given amount is introduced into pre-weighed reactor 1. The raw material is poured into raw material burette 4. The reactor is located inside furnace 2. The heating voltage is set using LATR 9, and two thermocouples 10, 10a, installed in the furnace and the reactor, are connected to the temperature regulators. The required temperature values of the process are set on the regulators. After the reactor heats up to a given temperature, the supply of raw materials through pump 3 is turned on. The raw materials from the burette enter the reactor, where, when interacting with the catalyst, the formation reactions of hydrogen-containing gas (a mixture of gases consisting of hydrogen (mainly), methane and ethane) and "non-hydrogen-containing" gas (a mixture of hydrogen gas free hydrocarbons, namely, non-reacting hexane and unsaturated hydrocarbons – hexenes and pentenes with different structure) occur. The obtained mixture of gases and unreacted raw materials after reactor 1 passes through condenser 5, in which the unreacted raw materials are condensed and transferred into pre-weighed receiving flasks 6, 7. Uncondensed gases are sent to gas valve 8 and

then collected in a special vessel. After turning off the heating of the furnace, the supply of raw materials is stopped. Based on the weight gain of the receiving flasks, the yield of the liquid product is determined, and the composition of this product is established by means of chromatography. Based on the readings of the gas meter and density, the output of the gas component is calculated. After cooling, the reactor with carbon material was unloaded, the obtained product was collected, weighed and its yield was calculated. The total amount of n-hexane used in this reaction was 400 ml or 264 g, and the reaction time was 8 h. The material balance of the process of thermal catalytic decomposition of n-hexane was determined: the amount of released gases was of 86.34 g (32.6%), liquid products – 162.62 g (61.6%) and carbon material – 15.04 g (5.7%).

3. Results and discussion

3.1. Studies of carbon materials composition and their physicochemical properties

As a first step, the elemental composition of the resulting CMs was established (Table 2). The high percentage of carbon (96.64%), as well as the rather low percentage of hydrogen (0.55%) in the obtained carbon material indicates a high content of carbon nanotubes in the resulting material.

To determine the fine structure of the resulting material, scanning electron microscopy (SEM) studies were carried out (Figure 2A, B, S2–S4). The most representative SEM images of the abovementioned carbon material at different magnifications are presented in Figure 2A, B. According to the obtained data, a fibrous structure of the surface of the film of the resulting carbon material can be clearly seen. In addition, based on the SEM data one may conclude that the obtained carbon materials consist mainly of multi-walled carbon nanotubes (MWCNTs) with diameters of 20–85 nm and lengths varying from 500 nm to 600 nm.

The results of energy-dispersive X-ray spectroscopy of the obtained carbon material (Figures 3A-C) indicate the presence of as high as 99.9% carbon in (Figures 3A, C), as well as the presence a small amount (0.1%) of nickel (Figure 3B, C), which was consistent with the data obtained by means of Raman spectroscopy (Figure 4). Most probably, the presence of nickel is due to the use of its salt as a catalyst in the obtaining of the abovementioned carbon material.

Figure 4 shows the Raman spectrum of the resulting CM. The presence of an absorption band of nickel in a region of 1100 cm^{-1} was observed, and this result corresponded well to the Raman microscopy database. In addition, characteristic peaks of the absorption of C=C bonds in the region of 1500 cm^{-1} and characteristic peaks of the absorption of CH bonds in the region of 2400 cm^{-1} were observed.

3.2. Electrochemical studies by using field-effect transistor setup
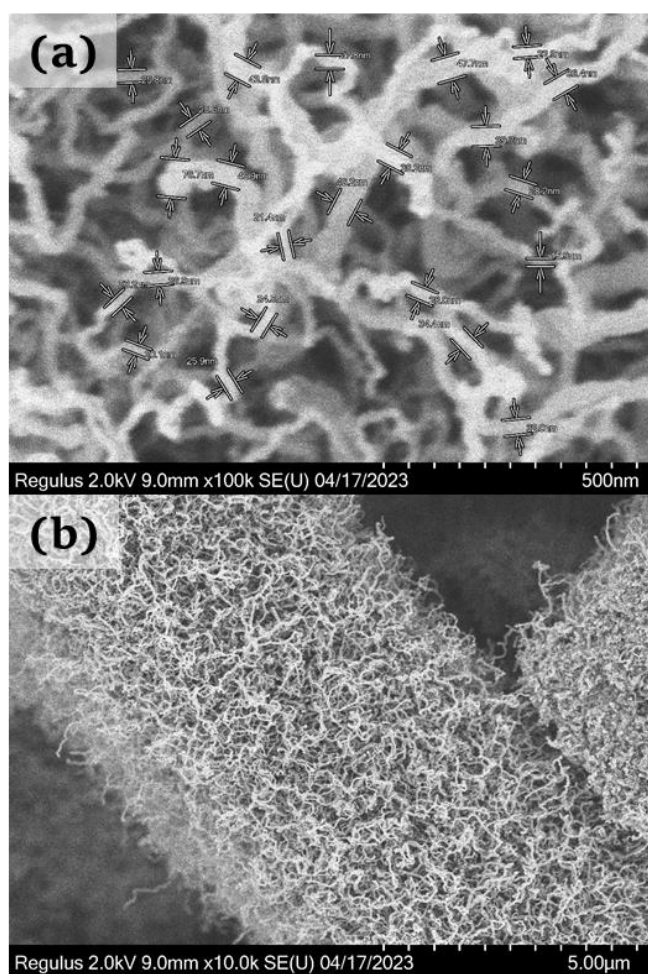
The most promising application of carbon materials is molecular electronics [34]. Therefore, as a last step, in order to study the applicability of the investigated materials, a field-effect transistor setup was fabricated.

Table 2 Elemental composition of the obtained carbon material.

Raw material	Conditions	Elemental analysis data		
		C, %	H, % N%	Ni, %
n-hexane	50 mL/h, 500 °C	96.64	0.55　0.16	0.1
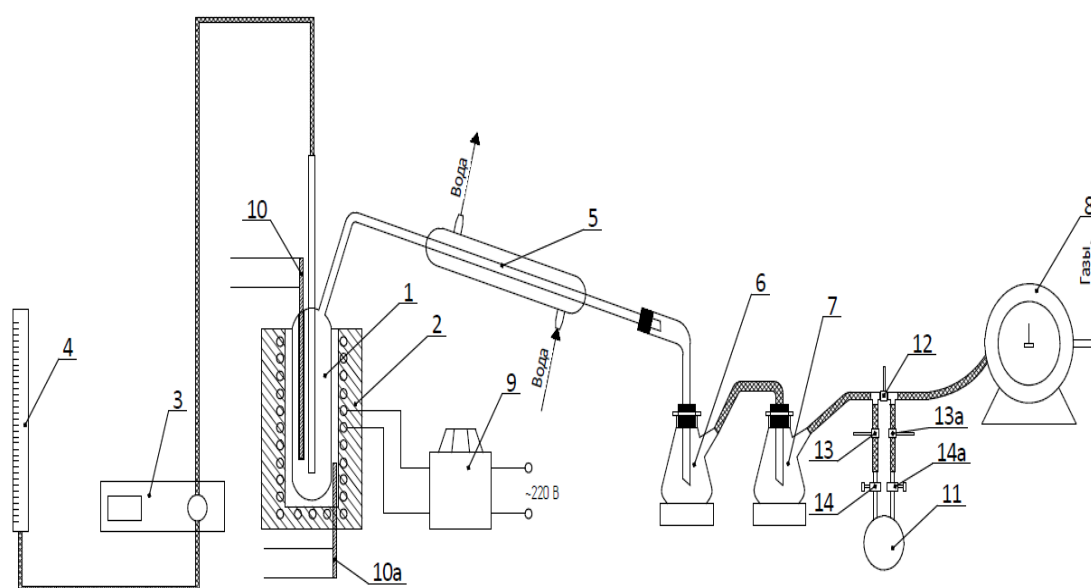
Figure 1 Laboratory setup for obtaining nanofibrous carbon/MWCNTs: 1 – reactor; 2 – oven; 3 – pump; 4 – raw burette; 5 – condenser; 6 – receiving flask; 7 – intermediate flask; 8 – gas valve; 9 – laboratory transformer (LATR); 10, 10a – thermocouples; 11 – pycnometer; 12 – middle clamp; 13, 13a – extreme clamps; 14, 14a – pycnometer taps.
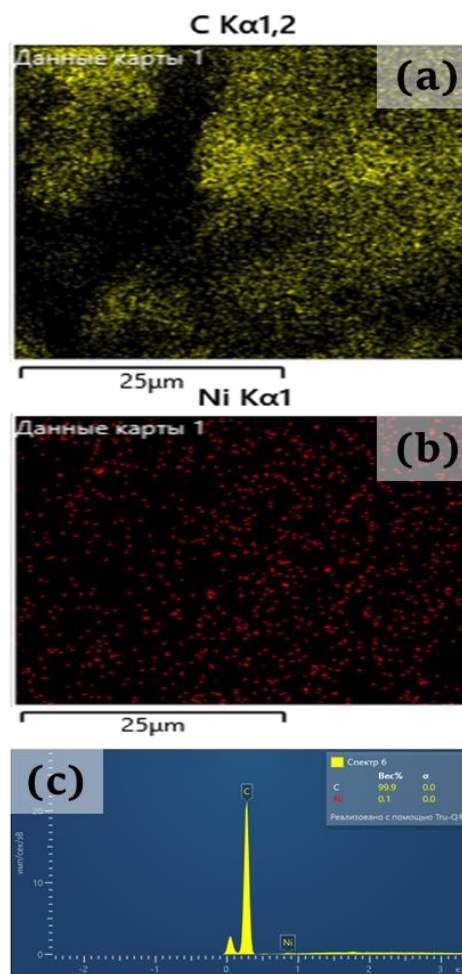
Figure 2 SEM images of the obtained carbon material: 500 μn increment (a); 5 μm increment (b).

Figure 3 Elemental mapping of MWCNTs: C (A), Ni (B). Chemical composition of the sample by means of energy-dispersive X-ray spectroscopy (C).

The transistor (Figure 5) was fabricated on a glass substrate, with a ready-made ITO film as a gate contact. The gate dielectric was made in the form of a thin film of aluminum oxide with a thickness of 390 nm by centrifugation from a solution at 1900 rpm and annealing in an oven for 130 min at a temperature of 320 °C. The aluminum oxide solution was created as in the works [35–36]. Drain-source contacts were made of aluminum foil with a thickness of 300 nm and deposited on top of the dielectric.

In the gap area W = 2 mm and L = 50 μm, a MWCNTs film with a thickness of 200 nm was deposited by means of thermal spraying in vacuum. The thickness of the aluminum oxide layer and MWCNTs was determined using a Nanoeducator II scanning probe microscope.

Current-voltage characteristics of OFET (Figure 6) were measured at room temperature under air atmosphere. From the figures of the current-voltage characteristics it is clear that with a positive voltage at the gate, an increase in currents of all types of transistors is observed, which corresponds to the electronic type of conductivity of the OFET transport channel. In this case, the dependences are nonlinear; there are practically no saturation areas in the output characteristics of the devices. The lack of a saturation in the output characteristics may be due to the presence of leakage currents.

Based on the current-voltage characteristics, the mobility of charge carriers was calculated using formula (2), equal to μ = 0.008 cm²·B⁻¹·c⁻¹ [37–38]:

$$\mu = \frac{I_{DS}}{\frac{W}{L} \cdot C \cdot \left(V_G - V_{th} - \frac{V_{DS}}{2}\right) \cdot V_{DS}}, \qquad (2)$$

where W is the channel width, L is the channel length, μ is the mobility, C is the capacitance per square area of the AlO$_x$ gate dielectric (for a thickness of 400 nm C = 8.9 nF/cm²), U_G is the gate voltage, U_{DS} is the voltage between drain and source, U_{th} – threshold voltage. The threshold voltage U_{th} was found from graphs of the dependence of the root of the current I_{DS} 1/2 on the voltage U_{DS} at U_G = const [39]. W = 2mm is the channel width, L = 50 μm is the channel length V_G = 30 V is the gate voltage, V_{DS} = 20 V is the voltage between drain and source, V_{th} = –12 V – threshold voltage. The obtained values are comparable with similar data [40–41] for transistors based on C60 fullerene and PCBM.

Based on the given values of charge carrier mobility, the maximum switching frequency for the developed transistor structures can be calculated using the formula [42]:

$$f = \frac{1}{2\pi}\frac{\mu V_{DS}}{L^2}, \qquad (3)$$

where L is the length of the transport channel, V_{DS} is the drain-source voltage, m is the carrier mobility. The maximum switching frequency available for this type of transistor was found to be equal to 1018 Hz at V_{DS} = 20 V.

4. Limitations

Carrying out the process at temperatures below 450 °C results in the formation of carbon nanotubes in low yields. The reaction temperature of 500 °C and above was found optimal for obtaining carbon nanotubes in good yields.

5. Conclusions

In summary, an effective and affordable method for producing nanofibrous carbon (multi-wall carbon nanotubes, MWCNTs) by means of thermolysis of *n*-hexane in the presence of formed *in situ* nano-sized Ni catalyst. To obtain such catalyst its precursor, nickel 2-ethylhexanoate, was used. Upon heating in hydrocarbon media this precursor decomposes to form Ni nanoparticles, and these nanoparticles were found to catalyze efficiently the process of the formation of carbon nanotubes upon relatively mild conditions (T = 500 °C). The properties of thus obtained MWCNTs were studied by SEM, energy-dispersive X-ray spectroscopy and Raman microscopy. Based on the SEM results the diameters of MWCNTs were found to be 20–67 nm and their lengths were found to be 500–600 nm. These results confirm the efficiency of the above-mentioned simple and affordable approach for synthesizing MWCNTs by using readily affordable carbon sources and catalysts at relatively mild reaction conditions.

By using the abovementioned MWCNTs samples, field-effect transistors were fabricated and their current-voltage characteristics were measured. The charge carrier mobility of 0.008 sm^2 V^{-1} s^{-1} was observed. Based on results of electrochemical studies, the herein reported MWCNTs were confirmed to be promising materials for the molecular electronics.

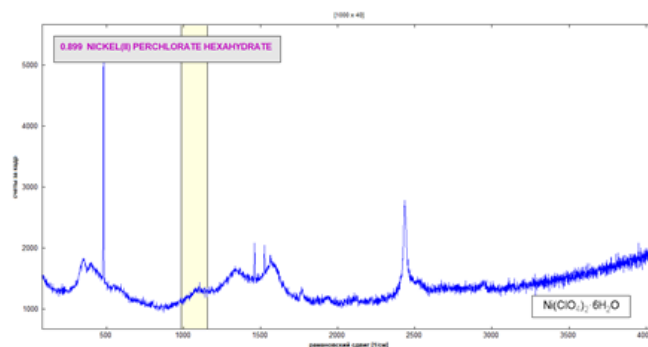## ● Supplementary materials

This manuscript contains supplementary materials, which are available on the corresponding online page. Figure S1: Enlarged picture of laboratory setup; Figures S2–S4: Enlarged pictures of SEM images of MWCTNs.
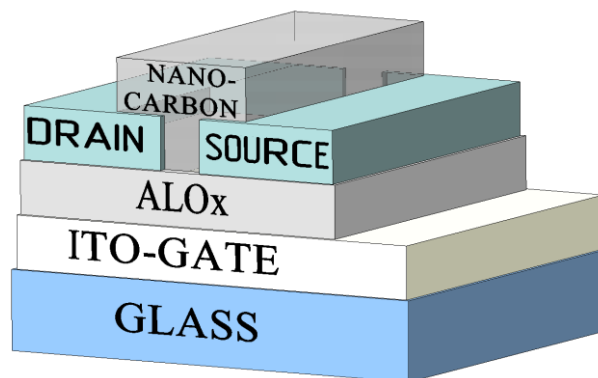
● Funding

● Acknowledgements

Figure 4 Raman spectrum of Nanofibrous carbon/MWCNTs at 300 K (excitation wavelength 532 nm).

Figure 5 Structure of the fabricated field-effect transistor.
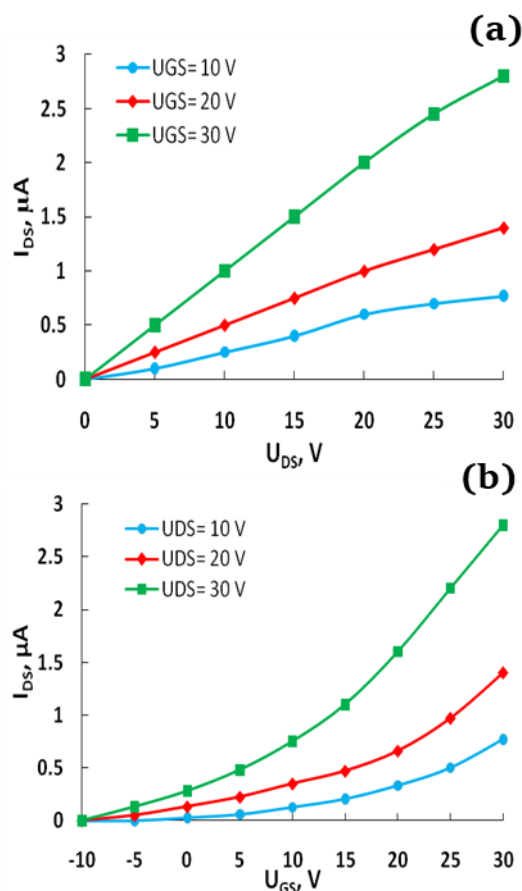
Figure 6 Current-voltage characteristics of OFET with a transport layer made of Nano-S: Output (a) transfer current-voltage characteristics of a transistor (b).

● Author contributions

Conceptualization: A.G.M., R.B.S.
Data curation: T.R.S., D.S.K., I.S.K.
Formal Analysis: I.A.M., A.F.A., R.N.G.
Funding acquisition: R.B.S., D.S.K., I.S.K.
Investigation: I.N.M., R.N.G.
Methodology: T.R.S.
Project administration: A.G.M., R.B.S.
Resources: A.F.A., D.S.K., I.S.K.
Software: I.N.M., I.A.M.
Writing – original draft: A.F.A., R.N.G.
Writing – review & editing: R.B.S., D.S.K., I.S.K.
Supervision: T.R.S.
Validation: I.N.M., A.F.A.
Visualization: T.R.S.

● Conflict of interest

The authors declare no conflict of interest.

● Additional information

Author IDs:
Ildar Mustafin, Scopus ID 57191665440;
Arslan Akhmetova, Scopus ID 7004645636;
Renat Salikhov, Scopus ID 11738898100;
Ilnur Mullagaliev, Scopus ID 57205464144;
Timur Salikhov, Scopus ID 55921773000;
Rail Galiakhmetov, Scopus ID 57191646671;
Olga V. Shabunina, Scopus ID 7801581388;
Igor S. Kovalev, Scopus ID 7102090085;
Dmitry S. Kopchuk, Scopus ID 14123383900;
Akhat G. Mustafin, Scopus ID 57191676129.

Websites:
Ufa State Petroleum Technological University, https://study.rusoil.net/;
Ufa University of Science and Technology, https://study.uust.ru/;
Ural Federal University, https://urfu.ru/en/;
I. Ya. Postovsky Institute of Organic Synthesis, Ural Branch of the RAS, https://iosuran.ru/.

References

1. Mishchenko SV, Tkachev AG. Carbon nanomaterials. Production, properties, application. Mashinostroenie. 2008; 320.
2. Mahato B, Lomov SV, Shiverskii A, Owais M. A review of electrospun nanofiber interleaves for interlaminar toughening of composite laminates. Polymers. 2023;15(6):1380 doi:10.3390/polym15061380
3. Lan G, Yang J, Ye RP, Boyjoo Y, Liang J, Liu X, Qian K. Sustainable carbon materials toward emerging applications. Small Methods. 2021;5(5):2001250. doi:10.1002/smtd.202001250
4. Egoroov NV, Sheshin EF. Carbon-based field emitters: properties and applications. Modern Develop Vacuum Electron Sources. 2020;449–528.
5. Liu Y, Kumar S. Polymer/carbon nanotube nano composite fibers–a review. ACS Appl Mater Interfaces. 2014;6(9):6069–6087. doi:10.1021/am405136s
6. Kirmani MH, Jony B, Gupta K, Kondekar, Ramachandran J, Arias-Monje PJ, Kumar S. Using a carbon fiber sizing to tailor the interface-interphase of a carbon nanotube-polymer system. Composites Part B Engineering. 2020;247:110284. doi:10.1016/j.compositesb.2022.110284
7. Newcomb BA, Giannuzzi LA, Lyons KM, Gulgunje PV, Gupta K, Liu Y, Kumar S. High resolution transmission electron microscopy study on polyacrylonitrile/carbon nanotube based carbon fibers and the effect of structure development on the thermal and electrical conductivities. Carbon. 2023;93:502–514. doi:10.1016/j.carbon.2015.05.037
8. Karakashov B. Studies of fibrous carbons for high-temperature thermal energy storage (Doctoral dissertation, Université de Lorraine). 2019.
9. Kour R, Arya S, Young S-J, Gupta V, Bandhoria P, Khosla A. Review—Recent advances in carbon anomaterials as electrochemical biosensors. J Electrochem Soc. 2020;167:037555. doi:10.1149/1945-7111/ab6bc4
10. Nurmukhametova A, Zenitova L. Carbon fiber. Overview. Norwegian Journal of development of the International Science. 2022;86:64–96.
11. Mukhina TN, Barabanov NL, Babash ES et al. Pyrolysis of hydrocarbon raw materials, Chemistry. 1987; 240.
12. Popov MV, Golovakhin VV, Gudyma TS, Lazarenko NS, Lapekin NL, Shestakov AA, Bannov AG. A method for producing carbon nanomaterial and hydrogen (options) and a device for producing carbon nanomaterial and hydrogen in a continuous mode. Patent RU №. 2790169, 2023 (in Russian) [Popov MV, Golovakhin VV, Gudyma TS, Lazarenko NS, Lapekin NI, Shestakov AA, Bannov AG. Sposob poluche-niya uglerodnogo nanomateriala i vodoroda (varianty) i ustroystvo dlya polucheniya uglerodnogo nanoma-teriala i vodoroda v nepreryvnom rezhime. Patent RF №2790169, 2023].
13. Avdeeva LB, Goncharova OV, Kuvshinov GG et al. Method for producing hydrogen and carbon material applicant and patent holder: Institute of Catalysis named after. Patent RU № 2064889 (in Russian) 1996; [Avdeyeva LB, Goncharova OV, Kuvshinov GG i dr.; Sposob polucheniya vodoroda i uglerodnogo materiala: Patent RF № 2064889,1996.]
14. Ermakova MA, Ermakov DYu, Kuvshinov GG, Plyasova LM. New Nickel Catalysts for the Formation of Filamentous Carbon in the Reaction of Methane Decomposition. J Catal. 1999;187:77–84. doi:10.1006/jcat.1999.2562
15. Marina A, Ermakova, Dmitriy Yu, Ermakov, Chuvilin A. et al. Decomposition of methane over iron catalysts at the range of moderate temperatures: the influence of structure of the catalytic systems and the reaction conditions on the yield of carbon and morphology of carbon filaments. J Catalysis. 2001;201:183–197. doi:10.1006/jcat.2001.3243
16. Reshetenko TV, Avdeeva LB, Ismagilov ZR et al, Carbon capacious Ni-Cu-Al$_2$O$_3$ catalysts for high-temperature methane decomposition. Appl Catalysis A Gen. 2003;247:51–63. doi:10.1016/S0926-860X(03)00080-2
17. Kuvshinov GG, Zavarukhin SG, Mogilnykh YuL et al. Implementation of the process for producing granular catalytic fibrous carbon on a pilot reactor scale, Chemical Industry.1998;5:300–307 p. (in Russian) [Kuvshinov GG, Zavarukhin SG, Mogil'nykh YUL i dr., Realizatsiya protsessa polucheniya granulirovannogo kataliticheskogo voloknistogo ugleroda v masshtabe pilotnogo reaktora, Khimicheskaya promyshlennost'. 1998; № 5. s. 300-307].
18. Steinfeld A, Kirillov V, Kuvshinov G et al. Production of filamentous carbon and hydrogen by solarthermal catalytic cracking of methane. Chem Eng Sci. 1997:3599–3603. doi:10.1016/S0009-2509(97)00166-8
19. Kuvshinov GG, Parmon VN, Sadykov VA, Sobyanin VA. New catalysts and catalytic processes to produce hydrogen and syngas from natural gas and other light hydrocarbons. Studies Surface Sci Catalysis. 1998;19:677.
20. Yu T, Li J, Yao J, Kang L. Qingwen Li. Filled carbon-nanotube heterostructures: from synthesis to application. Microstructures. 2023; doi:10.20517/microstructures

21. Karousios N, Tagmatarchis N, Tasis D. Current Progress on the Chemical Modification of Carbon Nanotubes. Chem Rev. 2010;110:5366–5397.

22. MacKenzie KJ, Dunens OM, Harris AT. An Updated Review of Synthesis Parameters and Growth Mechanisms for Carbon Nanotubes in Fluidized Beds. Ind Eng Chem Res. 2019;49(11):5323–5338. doi:10.1021/ie9019787

23. See CH, Harris AT. A review of carbon nanotube synthesis via fluidized-bed chemical vapor deposition. Ind Eng Chem Res. 2007; 46(4):997–1012. doi:10.1021/ie060955b

24. Ermakova M, Ermakov D, Kuvshinov G et al. Decomposition of methane over iron catalysts at the range of moderate temperatures: the influence of structure of the catalytic systems and the reaction conditions on the yield of carbon and morphology of carbon filaments. 2001;201:183–197. doi:10.1006/jcat.2001.3243

25. Reshetenko T, Avdeeva L, Ismagilov Z et al. Catalytic filamentous carbons-supported Ni for low temperature methane decomposition. 2005;102:115–120. doi:10.1016/j.cattod.2005.02.011

26. Reshetenko TV, Avdeeva LV, Ushakov VA et al. Coprecipitated iron-containing catalysts (Fe-Al$_2$O$_3$, Fe-Co-Al$_2$O$_3$, Fe-Ni-Al$_2$O$_3$) for methane decomposition at moderate temperatures: Part II. Evolution of the catalysts in reaction. Appl Catalysis A Gen. 2004;270:87–99. doi:10.1016/j.apcata.2004.03.045

27. Reshetenko T, Avdeeva L, Ismagilov Z et al. Catalytic Filamentous Carbon: Structural and Textural Properties. Carbon. 2004;42:2501–2507. doi:10.1016/S0008-6223(03)00115-5

28. Takenaka S, Kobayashi HO. Ni/SiO$_2$ catalyst effective for methan e decomposition into hydrogen and carbon nanofiber, J Catalysis. 2003;136:79–87. doi:10.1016/S0021-9517(02)00185-9

29. Ermakova M, Ermakov D. Ni/SiO$_2$ and Fe/SiO$_2$ catalysts for production of hydrogen and filamentous carbon via methane decomposition. 2002;77:225–233. doi:10.1016/S0920-5861(02)00248-1

30. Hazr M, Croiset E, Hudgins RR et al., Experimental investigation of the catalytic cracking of methane over a supported Ni catalyst. Can J Chem Eng. 2009;87:99–105. doi:10.1002/cjce.20087

31. Takenaka S, Shigeta Y, Tanabe E, Otsuka K. Methane decomposition into hydrogen and carbon nanofibers over supported Pd-Ni catalysts. J Catalysis. 2003;220:468–477. doi:10.1016/S0021-9517(03)00244-6

32. Mustafin IA, Galiakhmetov RN, Kurochkin AK, Akhmetov AF, Khanov AR. Termodestructive distillation of gas oil and fuel oil in the presence of ultrafine, metal-containing catalytic systems in pilot conditions. Chem Technol Fuels Oils. 2022;3:5–9. doi:10.32935/0023-1169-2022-631-3-5-9

33. Mustafin AG Galiakhmetov RN, Sudakova OM, Mustafin IA, Gimadieva AR. Method of producing nickel 2-ethylhexanoate. Patent holder: Bashkirskij gosudarstvennyj university. named after. Patent RU № 2612220 (in Russian) 2015; [Mustafin AG, Galiakhmetov RN, Sudakova OM, Mustafin IA, Gimadieva AR; Sposob polucheniya 2-ethylhexanoata nickelj: Patent RF № 2612220, 2015.]

34. Kamran U, Heo Y-J, Won Lee J, Park S-J. Functionalized Carbon Materials for Electronic Devices: A Review. Micromachines. 2019;10(4):234. doi:10.3390/mi10040234

35. Kim SH, Kang I, Kim YG, Hwang HR, Kim YH, Kwon SK, Jang J. High performance ink-jet printed diketopyrrolopyrrole-based copolymer thin-film transistors using a solution-processed aluminium oxide dielectric on a flexible substrate. J Mater Chem C. 2013;1(13):2408–2411. doi:10.1039/C3TC00718A

36. Avis C, Hwang HR, Jang J. Effect Of Channel Layer Thickness On The Performance Of Indium–Zinc–Tin Oxide Thin Film Transistors Manufactured By Inkjet Printing. ACS Appl Mater Interfaces. 2014;6(14):10941-10945. doi:10.1021/am501153w

37. Zhou Y, Wang X, Dodabalapur A. Dual-Band Perovskite Bulk Heterojunction Self-Powered Photodetector for Encrypted Communication and Imaging. Adv Electron Mater. 2022;2200786. doi:10.1002/adom.202200786

38. Tameev AR, Rakhmeev RG, Nikitenko VR, Salikhov RB, Bunakov AA, Lachinov AN, Vannikov A.V. Effect of excessive pressure on the drift mobility of charge carriers in poly(diphenylene phthalide) films. Phys Solid State. 2011;53:195–200. doi:10.1134/S106378341101032X

39. Zhou X, Wang Z, Song R, Zhang Y, Zhu L, Xue D. High performance gas sensors with dual response based on organic ambipolar transistors. J Mater Chem C. 2020;219(5):1584–1592. doi:10.1039/D0TC04843G

40. Kobayashi S, Takenobu T, Mori S, Fujiwara A, Iwasa Y. Sci Technol Adv Mat. 2003; 4. 371. doi:10.1016/S1468-6996(03)00064-0

41. Park B. Dielectric relaxation dependent memory elements in pentacene[6, 6]-phenyl-C61-butyric acid methyl ester bilayer field effect transistors. Thin Solid Films. 2015; 578. 156–160. doi:10.1016/j.tsf.2015.02.043

42. Köhler A, Bässler H. Electronic Processes in Organic Semiconductors: An Introduction. Wiley Weinheim. 2015.